

## **Time Resolved Structural Evolution of Additive Processed Bulk Heterojunction Solar Cells**

**James T. Rogers<sup>‡</sup>, Kristin Schmidt<sup>‡§</sup>, Michael F. Toney<sup>§</sup>, Guillermo C. Bazan<sup>†\*</sup>, Edward J. Kramer<sup>‡#</sup>**

*<sup>†</sup>Center for Polymers and Organic Solids, Department of Chemistry & Biochemistry, University of California, Santa Barbara, California 93106*

*<sup>‡</sup>Department of Materials, University of California, Santa Barbara, California 93106*

*<sup>§</sup>Stanford Synchrotron Radiation Lightsource, SLAC National Accelerator Laboratory, Menlo Park, California 94025*

*<sup>#</sup>Department of Chemical Engineering, University of California, Santa Barbara, California 93106*

### **Supplemental Information**

#### *Generation of 3D sector plots from raw GIWAXS data:*

To simplify analysis of the large number of 2D data sets, raw GIWAXS data were first transformed into a series of 2D sector plots. Here, a sector plot is simply an alternative representation of the data in a Cartesian coordinate system in  $q$  and  $\chi$ . To perform this operation, the raw data collected on a 2D x-ray detector (Figure 1a) are first broken up into a large number of equally spaced radial and azimuthal bins. Within each bin, the average intensity is calculated and this value is used to represent the intensity of one pixel at the corresponding location of the sector plot. The resulting plots are three-dimensional data sets whose x-axis is polar angle  $\chi$ , y-axis is  $q$ , and z-axis (color) is intensity. Additional care has been taken in constructing these plots as the use of a two dimensional detector in the GIWAXS geometry misses a portion of reciprocal space near the out-of-plane (polar) direction (black region shown in 2D sector plots, and zero intensity region in the 3D sector plots). Sector plots simplify visualization of the out-of-plane and in-plane scattering components as a function of  $q$  (i.e. polar angle near  $0^\circ$  and  $\pm 90^\circ$  respectively), while enabling easy comparison between data sets. Three dimensional sector plots reduce some issues associated with the use of a color scale to represent intensity values, and are useful for comparing GIWAXS data with features that exhibit a wide range of scattered intensities. In addition, these representations permit scattered intensity arising from x-ray

reflection from the sample surface to be subtracted from the collected data, allowing scattered intensity at low angles to be more clearly illustrated.

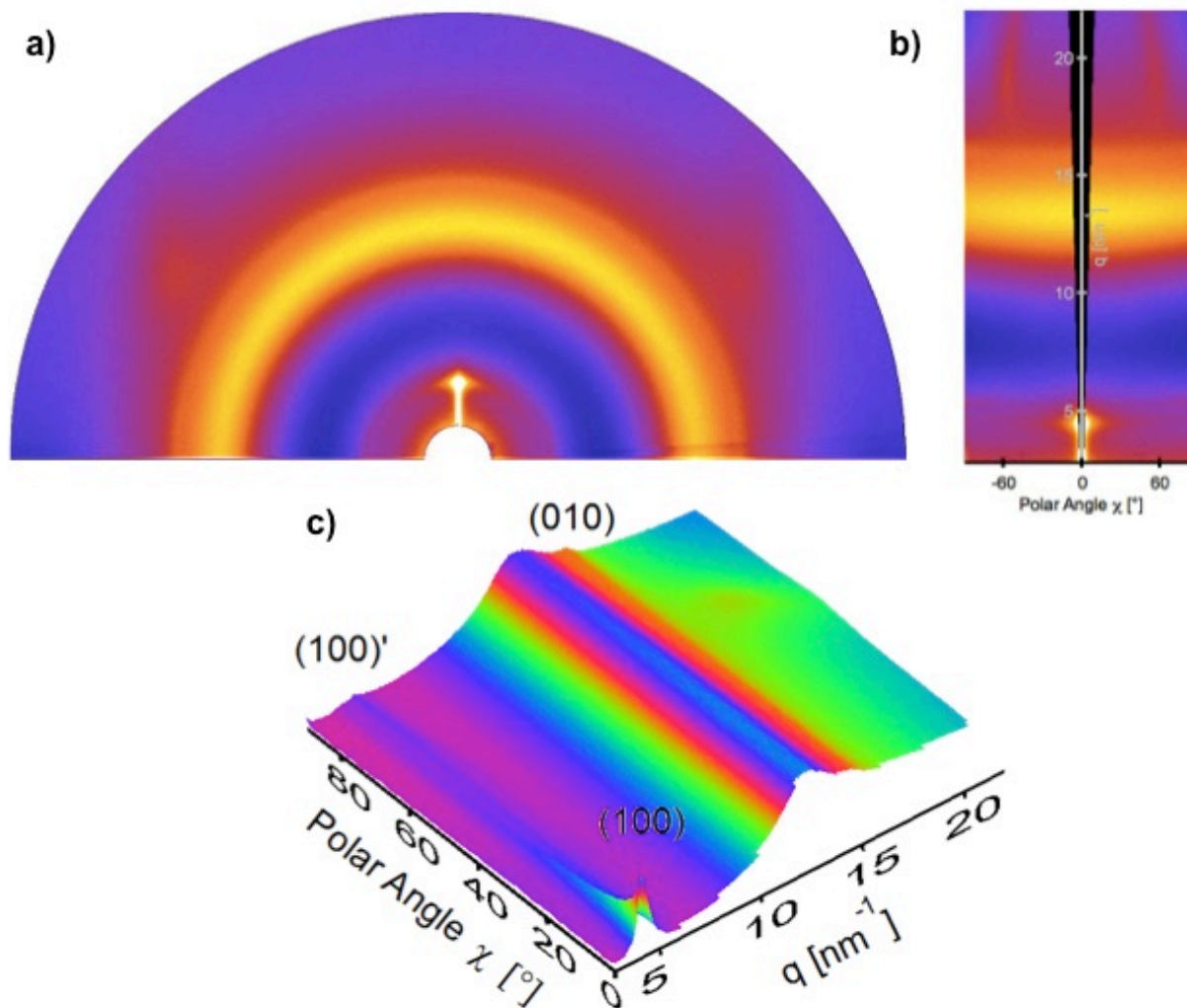


**Figure S1.** Transformation procedure for converting typical GIWAXS data from a 2D detector to the 3D presentation used in Figure 1. a) Raw GIWAXS data as collected on a 2D detector, b) the data transformed via radial and azimuthal binning into a 2D sector plot, c) data from the 2D sector plot represented in a 3D sector plot where changes in intensity are represented by changes in both height and color over only half the range of polar angles (i.e.  $-90^\circ$  to  $0^\circ$ ).

#### *GIWAXS of non-additive processed films:*

PCPDTBT:PC<sub>70</sub>BM films cast from a neat chlorobenzene solution are largely amorphous and show no evidence of structural evolution during the period of 2 to 78 minutes after spin coating.

Figure S2 shows the results of GIWAXS measurements made on PCPDTBT:PC<sub>70</sub>BM films represented as three dimensional sector plots. Figure S2a demonstrates the 3D sector plot generated from GIWAXS data taken on a PCPDTBT:PC<sub>70</sub>BM active layer cast from a pristine chlorobenzene solvent two minutes after spin coating. Figure S2b shows an identical measurement made 78 minutes after film deposition. Qualitative comparison reveals there is no significant temporal evolution in this system. Figure S2c shows the results of thermal annealing the same non-additive processed film for 20 minutes at 250°C, this figure demonstrates that the crystalline features characteristic of additive processed films are completely absent in non-additive processed films even after thermal annealing. However, it may be significant that the film cast from neat chlorobenzene only shows a very broad and low intensity peak at  $\sim 7 \text{ nm}^{-1}$  that is completely missing from the additive processed blend (Figure 1a). These results suggest that PCPDTBT forms an amorphous phase in polymer-fullerene blends processed without additives.

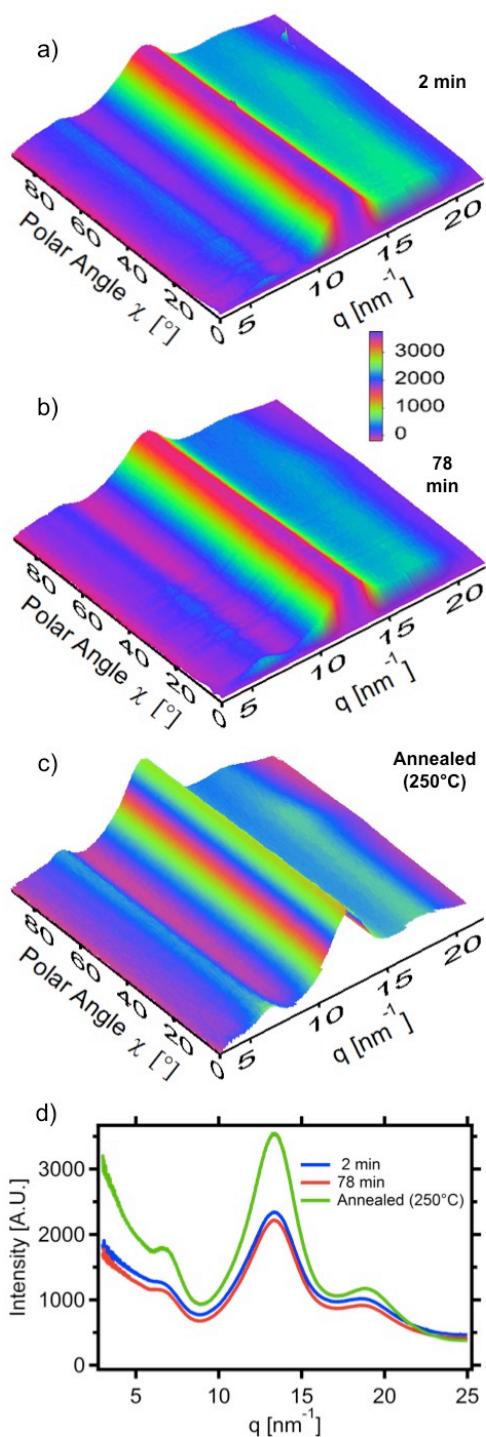


**Figure S2.** Three dimensional sector plot of a PCPDTBT:PC<sub>70</sub>BM thin film spin cast from pristine chlorobenzene solvent showing scattered intensity (on a linear scale) vs. polar angle  $\chi$  and scattering vector  $q$  (a) 2 min after spin coating, (b) 78 min after spin coating, (c) after annealing for 20 minutes at 250°C, and (d) integrated line scans of the raw GIWAXS data (over the full range of polar angles) highlighting the absence of structural changes during film drying and the absence of (100), (100)', and (010) features after annealing.

### Fitting GIWAXS Data:

Figure S3 more closely examines the time-dependent structural evolution of (100) and (100)' crystallites in PCPDTBT:PC<sub>70</sub>BM blends processed with 3% of the ODT additive. Here, line cuts taken near the out-of-plane ( $\chi=4^\circ$ ) and in-plane ( $\chi=82^\circ$ ) directions are used to demonstrate the shift in position, breadth, and intensity of the highly oriented (100) and (100)' alkyl chain stacking peaks (out-of-plane and in-plane represented on the same graph) as a function of time after casting.

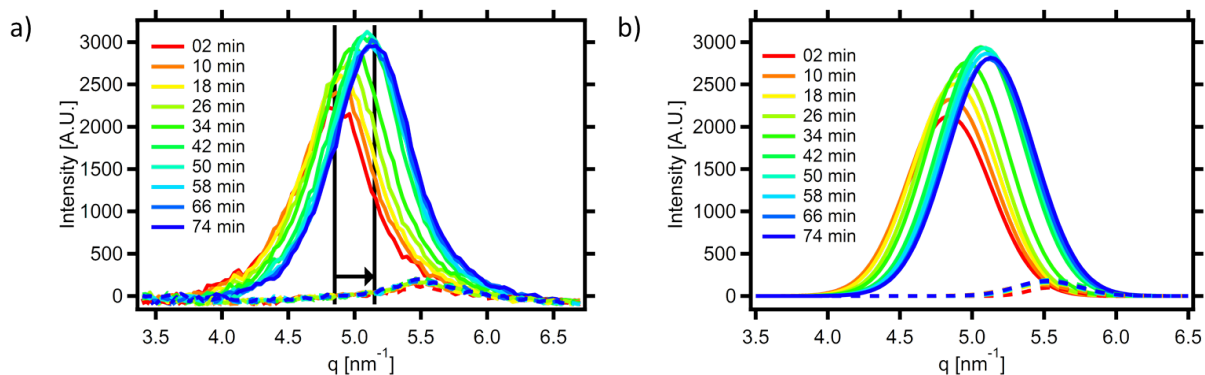


**Figure S3.** a) Raw data from out-of-plane (solid) and in-plane (dashed) line scans and b) the results of fitting out-of-plane line scans near the (100) peak ( $4.85 \text{ nm}^{-1} < q < 5.15 \text{ nm}^{-1}$ ) (solid) and in-plane line scans near the (100)' peak ( $q = 5.5 \text{ nm}^{-1}$ ) (dashed) which demonstrate the temporal evolution of (100) and (100)' scattering in a PCPDTBT:PC<sub>70</sub>BM film cast from a solution containing 3% ODT.

### Orientational order parameter calculation:

To analyze the orientational order of the polymer microstructure, line scans were taken at each polar angle and fit using a combination of Gaussian curves to represent the observed structural features (e.g. S3). The total scattered intensity (i.e. the area under each Gaussian curve), determined from this fit, was then plotted as a function of polar angle and a geometrical correction was applied to these values to account for the sinusoidally decreasing total scattered intensity observed with increasing polar angle as a result of the GIWAXS sample geometry (Figure S4).<sup>1</sup> Separate molecular orientation parameters  $f_{\parallel}$  and  $f_{\perp}$  are used to represent the orientation of the polymer scattering along the plane of the film surface and along the axis normal to the surface respectively,<sup>2</sup> and are given by

$$f_{\perp} = \int_0^{\pi/2} \cos^2 \chi \times f(\chi) d\chi$$

and

$$f_{\parallel} = \frac{1 - f_{\perp}}{2}$$

The quasi-pole figure  $f(\chi)$ , the geometrically corrected scattering intensity vs polar angle, is normalized so that  $\int f(\chi)d\chi = 1$  and thus  $2f_{\parallel} + f_{\perp} = 1$ . A uniaxial order parameter  $S$  can then be defined as

$$S = \frac{1}{2} (3f_{\perp} - 1)$$

where  $S$  ranges from 1 (diffracting plane normal perfectly aligned with the substrate normal) to -0.5 (diffraction plane normal parallel to the plane of the surface). This treatment assumes that there is rotational isotropy about the substrate normal, a valid assumption for our films which have no preferred direction in the plane of the film.

Figure S4 is used to demonstrate the geometrically corrected non-normalized total scattered intensities for the PCPDTBT(100) peak and the amorphous scattering. The plots are shown non-normalized in order to demonstrate the increase in the total scattered intensity of the (100) peak, relative to the decrease in the total scattered intensity of the amorphous peak. Due to the geometry of the GIWAXS setup, the full range of polar angles (i.e. 0 to  $\pi/2$ ) cannot be observed,<sup>3</sup> and scattering at these missing angles is not accounted for in the total scattered intensity.

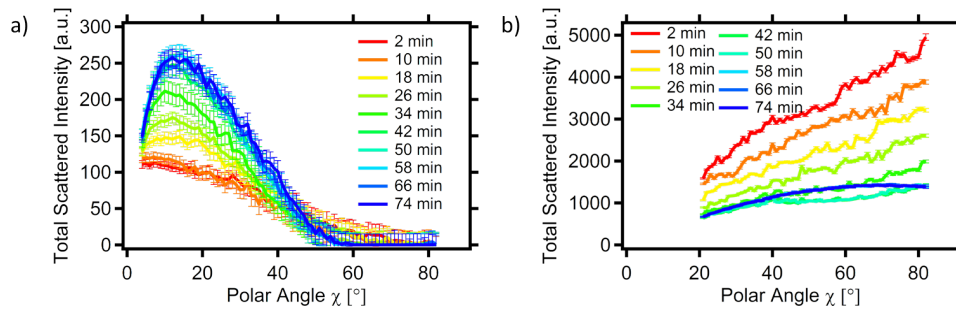


**Figure S4.** Geometrically corrected total scattered intensity (non-normalized) vs. Polar Angle for the (a) (100) and (b) amorphous scattering peaks, showing increases in the total scattered intensity from the (100) peak and decreasing total scattered intensity from the amorphous peak.

*Crystalline correlation length calculation:*

The correlation length of the (100) crystallites was estimated from the breadth of the Gaussian curve used to fit the (100) scattering feature according to

$$\text{Crystalline Correlation Length} = \frac{2\pi}{FWHM}$$

where FWHM represents the full width at half maximum of the Gaussian curve used to fit the scattering from the (100) feature. Figure S5 shows a slight decrease in the crystalline correlation length of the (100) peak as a function of time after casting.

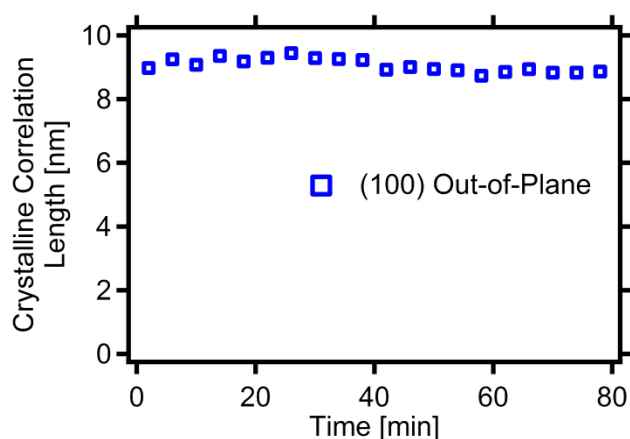


**Figure S5.** The crystalline correlation length for the (100) peak measured in the out of plane direction.

References:

- (1) Roe, R. J. *Methods of X-ray and neutron scattering in polymer science*; Oxford University Press: New York, 2000.
- (2) Li, X. F.; Andruzzi, L.; Chiellini, E.; Galli, G.; Ober, C. K.; Hexemer, A.; Kramer, E. J.; Fischer, D. A. *Macromolecules* **2002**, *35*, 8078.
- (3) Baker, J. L.; Jimison, L. H.; Mannsfeld, S.; Volkman, S.; Yin, S.; Subramanian, V.; Salleo, A.; Alivisatos, A. P.; Toney, M. F. *Langmuir* **2010**, *26*, 9146.